EPR and optical spectra of Yb^{3+} in $CsCdBr_3$: Charge-transfer effects on the energy-level structure of Yb^{3+} in the symmetrical pair centers

B. Z. Malkin, A. M. Leushin, and A. I. Iskhakova
Physics Department, Kazan State University, Kazan 420008, Russian Federation

J. Heber, M. Altwein, and K. Moller
Darmstadt University of Technology, Darmstadt D-64289, Germany

I. I. Fazlizhanov and V. A. Ulanov
Kazan Physical-Technical Institute, Kazan 420029, Russian Federation
(Received 24 February 2000)

Electron paramagnetic resonance (EPR), optical absorption, fluorescence, and excitation spectra of $CsCdBr_3$:1% Yb^{3+} single crystals were taken at 4.2 K. An analysis of the dependence of the EPR spectrum on the magnetic-field direction and a comparison of the recorded signal shapes with simulated envelopes over the magnetic dipole transitions of the expected dimers containing all ytterbium isotopes were performed. This allowed us to assign the measured EPR spectra unambiguously to the symmetrical pair center of the type Yb^{3+}-Cd^{2+} vacancy-Yb^{3+} substituting for three adjacent Cd^{2+} ions in the bromine octahedra chains. A distance of 0.596 nm between the magnetically equivalent Yb^{3+} ions was determined from the line splitting due to magnetic dipole-dipole interaction. An interpretation of the optical spectra in compounds containing $(YbBr_6)^{3-}$ complexes is presented, which is based on a crystal-field theory accounting for an interaction between the ground $4f^{13}(Yb^{3+})[4p^6(Br^-)]_6$ and excited $4f^{14}(Yb^{2+})4p^5(Br)[4p^6(Br^-)]_5$ charge-transfer configurations. The observed large splitting of the excited $^2F_{5/2}(4f^{13})$ crystal-field multiplet is explained on the basis of a quasiresonant hybridization of the $4f$-hole state with the spin orbitals of the charge-transfer states. With physically reasonable values of the fitted model parameters, the calculated energy level diagram of the $4f^{13}$ configuration and the g tensor of the Yb^{3+} ion in the crystal-field ground state are in good agreement with the experimental data.

I. INTRODUCTION

Doped with trivalent rare-earth (RE) ions the diamagnetic double bromide $CsCdBr_3$ is extensively studied in many laboratories as a promising material for upconversion lasers. The effective upconversion is due to the specific dimer structure of the RE centers in this compound. Of further interest are some peculiarities of the crystal-field (CF) splitting in the octahedral environment $(REBr_6)^{3-}$ [RE=Tm^{3+}, Yb^{3+}] as in $CsCdBr_3$,[1,2] $Cs_3Yb_2Br_9$,[3] and bromo elpasolites,[4] which cannot be interpreted in the framework of conventional CF theory. A fundamental understanding of the interactions between the localized $4f$ electrons and the crystal lattice is necessary to explain the unusual CF splittings as well as to elucidate the role of electronic excitations of the host crystal in nonradiative relaxation[5] and fast quantum upconversion[6] of RE ions in the double bromides.

The crystal lattice of $CsCdBr_3$ belongs to the D_{6h}^4 space group. It consists of linear chains of face-sharing slightly deformed $(CdBr_6)^{4-}$ octahedra arranged along the crystallographic c axis and connected through parallel chains of Cs^+ ions. Electron-paramagnetic-resonance (EPR) spectra of $CsCdBr_3$ crystals doped with Kramers [Gd^{3+} (Ref. 7)] and non-Kramers [Ho^{3+}, Tm^{3+} (Ref. 8)] ions taken in the microwave and submillimeter ranges of wavelengths, respectively, gave direct evidence that the RE^{3+} ions preferentially form charge compensated symmetric dimer centers of the type (RE^{3+}-Cd^{2+} vacancy-RE^{3+}) substituting for three adjacent Cd^{2+} ions in the chain (the point symmetry at the RE sites is C_{3v}). However, several other RE^{3+} minority centers of trigonal and C_s symmetry were identified in the optical and EPR spectra,[6,8–14] too. In particular, it was supposed that trigonal dimer centers of the asymmetric type (RE^{3+}-RE^{3+}-Cd^{2+} vacancy) are formed as well with a spectrum of the central RE^{3+} ion very similar to that of the symmetric dimers.[10,13] The existence of these asymmetric pair centers, which might play an essential role in quantum upconversion due to the close proximity of the RE ions, could not be proved by EPR spectra.[8,14] From calculations of the local lattice structure and from estimates of the CF parameters[1] it follows that the crystal fields in the symmetric and asymmetric dimers should differ substantially, a fact which could not be proved experimentally. Some of the observed spectral lines can be identified with quasi-single-ion centers of the type (RE^{3+}-Cd^{2+} vacancy-Cd^{2+}-RE^{3+}).[14]

For Eu^{3+},[13] Ho^{3+},[11] Pr^{3+},[15] Nd^{3+} and Er^{3+},[16] the energies and symmetries of a large number of the CF states, determined by polarized site-selective laser spectroscopy of the symmetric pair centers, were successfully described in the framework of conventional CF theory. However, considering the CF states of Tm^{3+}, the authors of Ref. 1 had to introduce term-dependent CF parameters. To describe the measured energy-level pattern of the $^1G_4$ CF multiplet, it was necessary to use parameters of the one-particle CF Hamil-

tonian that were about two times larger than the corresponding parameters obtained from the splittings of all other CF multiplets. The difference between the measured total splitting of the $^1G_4$ multiplet and the calculated one with the parameters from the other multiplets is so large ($\approx 150\ cm^{-1}$) that it cannot be attributed to any known correction of the one-particle CF model (due to electron-phonon interaction or correlated CF, for example). In Ref. 1 it was proposed that this singular increase of the CF splitting of $^1G_4$ is caused by quasiresonant scattering of lattice excitons by the Tm^{3+} ions. However, no reasonable estimate for this effect was presented.

Generally, the most basic information about the CF experienced by RE ions in a given host lattice can be obtained from the theoretically most simple analysis of the Yb^{3+} spectra because in this case the one-particle approximation is approved (one hole in the electronic $4f$ shell). The absorption and emission spectra of $CsCdBr_3:Yb^{3+}$ were studied in Refs. 2 and 17 and an energy-level scheme of the Yb^{3+} ions in the symmetric dimers was proposed. But the CF states were not characterized by symmetry and no attempts were made to analyze them in terms of a set of CF parameters.

In this paper, EPR as well as optical absorption, fluorescence, and excitation spectra of $CsCdBr_3:Yb^{3+}$ were taken at liquid-helium temperature. The EPR signals could unambiguously be identified as magnetic dipole transitions between the Zeeman components of the ground state of the symmetric dimers by their specific dependence on the magnetic-field direction and by the hyperfine structure due to the odd ytterbium isotopes. The measured g factors of the ground state and the CF energies of the Yb^{3+} ions are analyzed in terms of a semiempirical model taking into account the configuration mixing ($4f^{13}$,$4f^{12}5d^1$) by the odd CF as well as the quasiresonant mixing of the ground configuration $4f^{13}(Yb^{3+})[4p^6(Br^-)]_6$ with the 36 symmetrized molecular spin orbitals of the charge-transfer configuration $4f^{14}(Yb^{2+})4p^5(Br)[4p^6(Br^-)]_5$. In earlier studies of charge-transfer effects on the CF splitting of $4f^n$ multiplets, the fine structure of the charge-transfer bands and their possible overlap with the excited states of the $4f^n$ configuration were not taken into account.[18] A systematic study of the charge-transfer bands of the lanthanide halides demonstrates a general trend of decreasing transfer energies with increasing charge of the RE nuclei and increasing size of the ligands (F-Cl-Br-I).[19] Thus, low energies for charge-transfer excitations in the $(YbBr_6)^{3-}$ complexes can be expected. We suppose that charge-transfer states can come into quasiresonance with the excited state $^2F_{5/2}(Yb^{3+})$ causing anomalous CF splittings of this state in the bromo elpasolites, $Cs_3Yb_2Br_9$ and $CsCdBr_3:Yb^{3+}$.

II. EXPERIMENTAL RESULTS

The experiments described below were performed on single crystals grown by the Bridgeman method. The procedure is described in Ref. 6.

A. EPR spectra and spin-Hamiltonian parameters

The EPR spectra in $CsCdBr_3:Yb^{3+}$(1 mol %) were taken at 4.2 K with an E 12 Varian spectrometer at the frequency

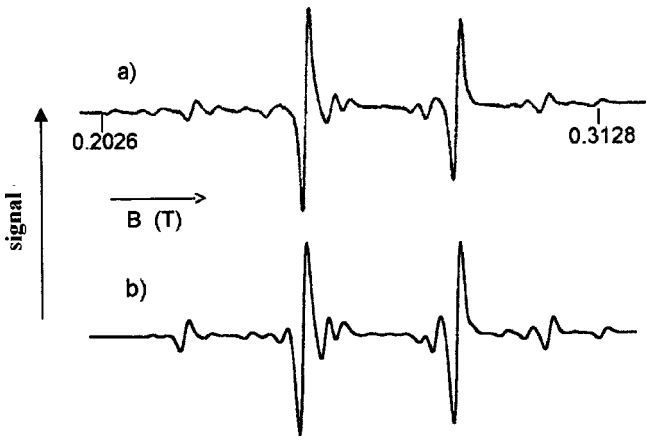

FIG. 1. Measured (a) and simulated (b) EPR spectra of $CsCdBr_3:Yb^{3+}$. Magnetic field $\mathbf{B}\|C_3$, $\nu = 9.282$ GHz, $T = 4.2$ K, $c = 1\%$.

$\nu = 9.282$ GHz and for static magnetic fields up to 1.3 T. The angular dependence of the spectra was studied rotating the sample around the microwave magnetic field $\mathbf{B}(t)$, which was fixed normal to the plane containing the static magnetic-field $\mathbf{B}$ and the crystallographic c axis.

There are three Yb isotopes, ^{170}Yb (nuclear spin $I = 0$), ^{171}Yb ($I = 1/2$), and ^{173}Yb ($I = 5/2$) with natural abundances of 69.5%, 14.3%, and 16.2%, respectively. The Yb^{3+} resonance signals are easily recognized by their characteristic hyperfine structure. The spectra measured in the magnetic-field range $\mathbf{B}$ from 0.20 to 0.32 T, contain two main lines and a large number of satellites with amplitudes 15 to 20 times smaller. The behavior of the intense lines under rotation of the magnetic field from $\mathbf{B}$ parallel to $\mathbf{B}$ perpendicular to the symmetry axis is typical for a spectrum of a pair of identical ions. The difference between the resonance fields of the two main lines is largest for the magnetic field $\mathbf{B}$ parallel to the c axis [Fig. 1(a)]. Increasing the angle between the magnetic field and the c axis, these lines move together and coincide at 54.5°. For $\mathbf{B}\perp c$ [Fig. 2(a)], the lines approach their second extremum position with half the distance between them as for $\mathbf{B}\|c$. The low-intensity satellite lines separate into two

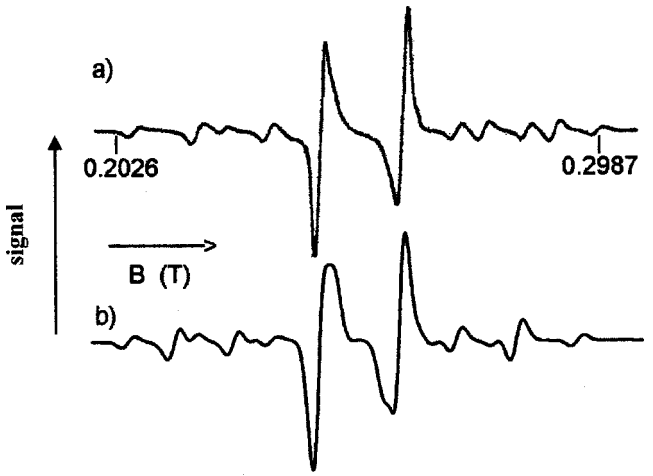

FIG. 2. Measured (a) and simulated (b) EPR spectra of $CsCdBr_3:Yb^{3+}$. Magnetic field $\mathbf{B}\perp C_3$, $\nu = 9.282$ GHz, $T = 4.2$ K, $c = 1\%$.

TABLE I. Ground state g factors and crystal-field energies (in cm^{-1}) of Yb^{3+} in the $(YbBr_6)^{3-}$ complexes.

	$Cs_2NaHoBr_6:Yb^{3+}$			$Cs_3Yb_2Br_9$		$CsCdBr_3:Yb^{3+}$				
		Theory			Theory	Experiment		Theory		
	Experiment[a]	$4f^{13}$	$+4f^{14}$Br	Experiment[b]	$4f^{13}$	Refs. 2 and 17	This paper	$4f^{13}$	$+4f^{12}5d^1$	$+4f^{14}$Br
1	2	3	4	5	6	7	8	9	10	11
$g_\parallel$		2.667	2.666		2.693		2.509 ± 0.004	2.634	2.523	2.540
$g_\perp$		2.667	2.666		2.640		2.614 ± 0.002	2.676	2.725	2.706
$^2F_{7/2}$ 1	$0\,\Gamma_6$	0	0	0	0	0	0	0	0	$0\,\Gamma_4$
$^2F_{7/2}$ 2	$215\,\Gamma_8$	188	215	114	142	114, 115	159	146	144	$161\,\Gamma_4$
$^2F_{7/2}$ 3				140	212	161, 167	198	200	201	$217\,\Gamma_{56}$
$^2F_{7/2}$ 4	$476\,\Gamma_7$	428	478	441	438	464	466	418	421	$461\,\Gamma_4$
$^2F_{5/2}$ 1	$10144\,\Gamma_8$	10 296	10 144	10 119	10 119	10 121, 10 122	10 125	10 280	10 277	$10\,120\,\Gamma_4$
$^2\Gamma_{5/2}$ 2				10 146	10 146	10 138	10 139	10 300	10 301	$10\,140\,\Gamma_{56}$
$^2F_{5/2}$ 3	$10\,629\,\Gamma_7$	10 586	10 623	10 590	10 438	10 596, 10 599	10 598	10 576	10 578	$10\,591\,\Gamma_4$

[a]Reference 4.
[b]Reference 3.

groups with line shifts correlated to the shift of one of the two main lines under rotation of the sample in the magnetic field. For low fields (0.12–0.15 T) an additional low-intensity signal appears (amplification increased up to 50) at finite angles between the magnetic field **B** and the c axis.

The ground state of the Yb^{3+} ion in $CsCdBr_3$ is well separated from the other CF states (see Table I). So, we can use the spin-Hamiltonian approximation to describe the EPR spectra. In the crystallographic system of coordinates, the spin-Hamiltonian of a dimer parallel to the crystal symmetry axis can be written as

$$H=H_1+H_2+K_\perp(S_{1x}S_{2x}+S_{1y}S_{2y})+K_\parallel S_{1z}S_{2z}, \quad (1)$$

where

$$H_i=g_\parallel\mu_B B_z S_{iz}+g_\perp\mu_B(B_xS_{ix}+B_yS_{iy})+A_iS_{iz}I_{iz} + B_i(S_{ix}I_{ix}+S_{iy}I_{iy})+V_i[3I_{zi}^2-I_i(I_i+1)] \quad (2)$$

is the spin-Hamiltonian of a single ion with the effective spin $S=1/2$ (we neglect here the nuclear Zeeman energy and small contributions nonlinear in the magnetic field and nuclear-spin components).[20] μ_B is the Bohr magneton, V_i is the quadrupole hyperfine constant, which is nonzero for the ^{173}Yb isotope.[21] $A=g_\parallel A_J/g_J$ and $B=g_\perp A_J/g_J$ are the magnetic hyperfine constants that are expressed through the known values of the magnetic hyperfine constants A_J of ^{171}Yb(887 MHz) and ^{173}Yb (-243.4 MHz),[21] and the Lande factor g_J in the free-ion ground state $^2F_{7/2}$.

The contributions to the Hamiltonian due to the magnetic dipole-dipole interaction in a dimer with distance R are given by[14]

$$K_\perp^{\rm dip}=\frac{(g_\perp\mu_B)^2}{R^3}, \quad K_\parallel^{\rm dip}=-2\frac{(g_\parallel\mu_B)^2}{R^3}. \quad (3)$$

The two most intense lines in the observed spectra are assigned to the dimers consisting of two equivalent $^{170}Yb^{3+}$ ions with zero nuclear moment. The simplicity of the corresponding spectra allows us to determine the spin-Hamiltonian parameters solely from the data for **B** parallel and perpendicular to the symmetry axis c. The four electronic states of the dimer are characterized by the total spin $S=0,1$ and its projection S_B on the direction of the magnetic field. For the magnetic field $\mathbf{B}\parallel c$ and the microwave field $\mathbf{B}(t)\perp\mathbf{B}$, magnetic dipole transitions are allowed ($\Delta S=0,\Delta S_B=\pm1$) at the resonance fields B_{z1} and B_{z2}, which satisfy the equations

$$2\pi\hbar\nu=g_\parallel\mu_B B_{z1}+(K_\perp-K_\parallel)/2;$$

$$2\pi\hbar\nu=g_\parallel\mu_B B_{z2}-(K_\perp-K_\parallel)/2. \quad (4)$$

For the magnetic field $\mathbf{B}\perp c$, transitions are allowed at the resonance fields B_{x1} and B_{x2} given by the equations

$$2\pi\hbar\nu=[(g_\perp\mu_B B_{x1})^2+(K_\perp-K_\parallel)^2 16]^{1/2}+(K_\perp-K_\parallel)/4, \quad (5)$$

$$2\pi\hbar\nu=[(g_\perp\mu_B B_{x2})^2+(K_\perp-K_\parallel)^2 16]^{1/2}-(K_\perp-K_\parallel)/4. \quad (6)$$

From the measured values of the resonance fields B_{xi} and B_{zi}, we can obtain the g factors of the Yb^{3+} ion in the ground-state doublet (Table I, column 8) and the anisotropic part of the interionic interaction $K_\perp-K_\parallel=(3975\pm5)\times10^{-5}\,cm^{-1}$. If we assume that the ions in the dimer are coupled by magnetic dipole-dipole interaction, we can obtain their interionic distance $R=0.5962$ nm from the value of the anisotropy constant $K_\perp-K_\parallel$. This value is consistent with the corresponding distances in the symmetric dimers of thulium (0.5943 nm),[1] holmium (0.5937 nm),[14] and gadolinium (0.593 nm).[7] The small increase of the interionic distances with decreasing ionic radii of the RE ions is consistent with calculations on the local deformation of the lattice structure.[1]

At the magnetic-field directions considered above, $\Delta S_B=\pm2$ transitions are strictly forbidden; but they become allowed (and have been observed) if the field **B** is inclined to the c axis. In agreement with the experimental results, the calculated maximum intensity of these transitions is about two orders of magnitude lower than the intensity of the allowed transitions at $\nu=9$ GHz. It is noteworthy that from these measurements we cannot find an exact value of a gap

between the singlet $S=0$ and triplet $S=1$ levels that may contain a contribution from isotropic exchange interaction.

We can present an additional confirmation of the observed EPR spectra as belonging to the symmetric pair centers by comparing the stimulated and recorded spectral envelopes. Assuming Gaussian line shapes for the individual electron-nuclear transitions with half-widths $(\ln 2)^{0.5}\delta B_{if}$ in a dimer containing $^{m}Yb^{3+}$ and $^{m'}Yb^{3+}$ ions, the shape of the corresponding EPR signal at the fixed frequency ν is given by

$$S_\nu(B|mm') = -\sum_{i,f} W_{if}(\mathbf{B}_{0,mm'}^{(if)})(B-B_{0,mm'}^{(if)})(\delta B_{if})^{-2} \times \exp\left[-\left(\frac{B-B_{0,mm'}^{(if)}}{\delta B_{if}}\right)^2\right]. \quad (7)$$

Here

$$W_{if}(\mathbf{B}_{0,mm'}^{(if)}) = |\langle i|g_\perp(S_{y1}+S_{y2})|f\rangle|^2 \quad (8)$$

is the relative integral intensity of the magnetic dipole transition between the initial (i) and final (f) electron-nuclear states of a dimer at the frequency ν induced by the ac magnetic field $B_y(t)$. $\mathbf{B}_{0,mm'}^{(if)}$ is the resonance magnetic field for this transition.

By numerical diagonalization of the Hamiltonian (1) for all dimers made up by all different isotope combinations (^{170}Yb-^{170}Yb, ^{170}Yb-^{171}Yb, ^{170}Yb-^{173}Yb, ^{171}Yb-^{171}Yb, ^{171}Yb-^{173}Yb, ^{173}Yb-^{173}Yb), we obtained the magnetic-field dependencies of the resonance frequencies and the relative integral intensities of all possible magnetic dipole transitions. The minimum rank of the Hamiltonian matrix is 4 for two $^{170}Yb^{3+}$ ions, the maximum rank 144 for two $^{173}Yb^{3+}$ ions. The values of the g factors used in the calculations are given in Table I. The corresponding magnetic hyperfine constants are $A(^{171}Yb)=1948$ MHz, $B(^{171}Yb)=2029$ MHz, $A(^{173}Yb)=-534$ MHz, and $B(^{173}Yb)=-557$ MHz. The quadrupole hyperfine constant $V(^{173}Yb)=-5.9$ MHz has been obtained from the electronic quadrupole moment of the CF ground state determined by means of the CF parameters presented in column 8, Table II. The contribution of the host lattice (point charge) to the quadrupole constant was estimated to be 0.1 MHz. The simulated spectral envelopes $S_\nu(B)$ in Figs. 1 and 2 represent sums over the spectra of all possible dimers with statistical weights determined by the concentrations $c(m)$ of the ytterbium isotopes:

$$S_\nu(B) = \sum_{mm'} \frac{c(m)c(m')S_\nu(B|mm')}{[2I(m)+1][2I(m')+1]}. \quad (9)$$

Varying only the widths of the individual electron-nuclear transitions (the final values $\delta B_{if}\cong 0.00135$ T for $\mathbf{B}\|c$ and 0.00185 T for $\mathbf{B}\perp c$ are close to the linewidths of the measured signal) we were able to reproduce very well the shapes of the measured spectra (compare Figs. 1 and 2). This result and the absence of any other intense EPR signal confirm that the Yb^{3+} ions, similarly to other RE^{3+} ions in $CsCdBr_3$, form preferentially symmetric dimer centers of the type [Yb^{3+}-Cd^{2+} vacancy-Yb^{3+}].

It was assumed in Ref. 2 that as much as 20% of the Yb^{3+} ions in $CsCdBr_3$ form asymmetric dimers with a significantly smaller interionic distance close to $c/2=0.34$ nm. We observed several additional unidentified EPR lines in the magnetic-field range from 0.05 to 0.45 T but all these signals were about two orders of magnitude weaker than the main EPR lines. It is possible that due to a large zero-field splitting (more than 60 GHz), induced by strong anisotropic exchange in the asymmetric dimers, one has to apply magnetic fields higher than 1.5 T to observe the corresponding EPR signals.

TABLE II. Crystal-field parameters (cm^{-1}) in (a) $CsCdBr_3$:RE^{3+} (symmetric pair centers), (b) $Cs_3Lu_2Br_9$:Er^{3+}, (c) $Cs_3Yb_2Br_9$, and (d) $Cs_2NaHoBr_6$:Yb^{3+}.

RE	Ho	Er		Tm	Yb		
B_p^k	a[a]	b[b]	a[c]	a[d]	c	d	a
1	2	3	4	5	6	7	8
B_2^0	−75.6	−130.6	−67.5	−81.4	−111.5	0	−68.4
B_4^0	−94.3	−106.4	−98.4	−82.0	−88.7	−84.6	−81.6
B_6^0	12.75	10.2	8.7	11.26	6.35	8.51	8.69
B_4^3	2841	3230	2993	2362	2333	2393	2323
B_4^{-3}	0	?	0	0	−127	0	0
B_6^3	216.2	174.5	209	153	57.9	105	58.9
B_6^{-3}	0	?	0	0	5.8	0	0
B_6^6	149.8	98.2	87.4	105.9	54	82	29.9
B_6^{-6}	0	?	0	0	−13.7	0	0

[a]Reference 14.
[b]Reference 26.
[c]Reference 16.
[d]Reference 1.

B. Optical spectra and the energy-level diagram

The theoretical discussion of Yb^{3+} spectra is much easier than of the other RE^{3+} ions because there are only 14 different quantum states in the $4f^{13}$ ground configuration. The free-ion ground-state $^2F_{7/2}$ and the excited state $^2F_{5/2}$ are split by the CF into four and three Kramers doublets, respectively, transforming according to the irreducible representations Γ_4 and Γ_{56} of the point symmetry double group C_{3v} of the RE^{3+} ions in the dimer centers.

From our studies of the absorption and excitation spectra of $CsCdBr_3$ doped with 1 mol % of ytterbium, we determined the energies of the CF sublevels of the excited state $^2F_{5/2}$ at 4.2 K (Table I, column 8) which are very close to the values given in Refs. 2 and 17. These energies are also very similar to those measured in $Cs_3Yb_2Br_9$ Ref. 3 (Table I, column 5) having a stoichiometric dimer structure with the Yb^{3+} ions in a sixfold bromine coordination closely resembling that of Yb^{3+} in $CsCdBr_3$.[22] The excitation spectrum of the total fluorescence (Fig. 3) shows several sharp lines and a broad vibronic sideband up to 10 800 cm^{-1}. The most pronounced peak is situated at ~10600 cm^{-1}. The insert shows the peak to consist of several lines yielding different fluorescence spectra (not presented here). Out of those excitation lines we selected the one at 10 598 cm^{-1} showing the best resolved fluorescence transitions with the least overlap with other lines.

The unpolarized fluorescence spectrum (Fig. 4) was taken at 4.2 K by laser excitation at 10 598 cm^{-1}. This spectrum

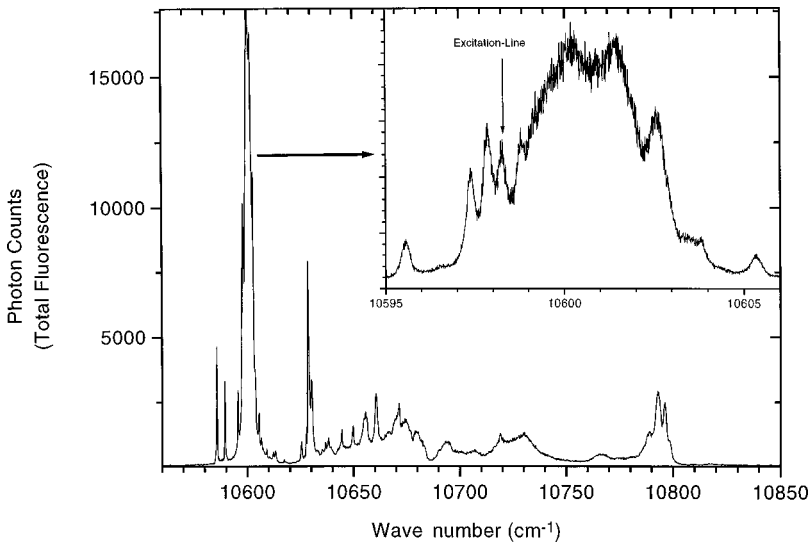

FIG. 3. Optical excitation spectrum of $CsCdBr_3:Yb^{3+}$, $T=4.2$ K, $c=1\%$.

contains three well-resolved lines corresponding to transitions from the lowest CF sublevel $1\Gamma_4$ of the excited state $^2F_{5/2}$ to the sublevels of the $^2F_{7/2}$ ground state (the irreducible representations of the energy levels were taken from CF calculations). The fluorescence line at 10 125 cm^{-1} is attributed to the transition to the CF ground state $^2F_{7/2}(1\Gamma_4)$. The doublet structured emission from the next higher Γ_{56} sublevel of $^2F_{5/2}$, observed at 15.5 K in Ref. 17, was absent in our spectra. The emission spectrum in the range from 9800 to 10 100 cm^{-1} has a very complicated structure (see Fig. 4). The zero-phonon transitions to the second $(2\Gamma_4)$ and third $(3\Gamma_{56})$ sublevel of $^2F_{7/2}$ are superimposed on the vibronic sideband of the transition to the lowest sublevel $(1\Gamma_4)$. The most intense line in this spectral region at 9966 cm^{-1} is assigned to the transition $^2F_{5/2}(1\Gamma_4)\rightarrow{}^2F_{7/2}(2\Gamma_4)$ and the line at the extreme left in this region (at 9927 cm^{-1}), which lies well behind the boundary of the phonon spectrum, is assigned to the $^2F_{5/2}(1\Gamma_4)\rightarrow{}^2F_{7/2}(3\Gamma_{56})$ transition. The lowest line at 9659 cm^{-1} reported by others[2,17] as well, is not shown in the spectrum. It is assigned to the $^2F_{5/2}(1\Gamma_4)\rightarrow{}^2F_{7/2}(4\Gamma_4)$ transition. Thus, our interpretation of the fluorescence spectrum differs remarkably from the one presented in Refs. 2 and 17 (columns 7 and 8, Table I). It is noteworthy that the authors of Refs. 2 and 17 followed Ref. 3, constructing the energy-level scheme of the $^2F_{7/2}$ CF multiplet in $Cs_3Yb_2Br_9$ (column 5, Table I), which disagrees with the theoretical models considered below.

III. CALCULATIONS OF THE ENERGY-LEVEL STRUCTURE

The Hamiltonian of an electron localized in the *nl* shell (*n* is the principal quantum number and *l* is the orbital angular momentum) of the Yb^{3+} ion can be written as follows:

$$H(nl)=E(nl)+H_{SO}(nl)+H_{CF}(nl), \tag{10}$$

where $E(nl)$ is the orbital energy, $H_{SO}(nl)$ is the Hamiltonian of the spin-orbit interaction, and $H_{CF}(nl)$ is the CF Hamiltonian. In principle, we can introduce two different spin-orbit interaction constants for impurity centers of trigonal symmetry:

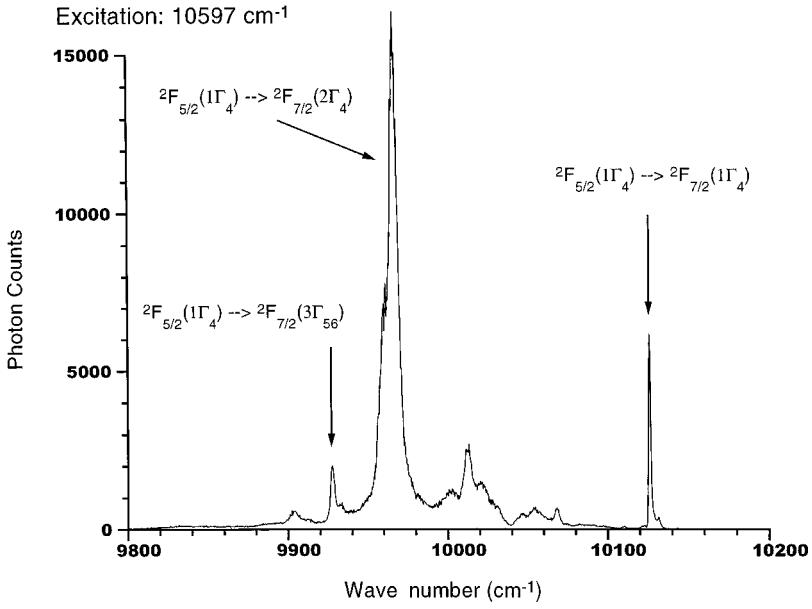

FIG. 4. Fluorescence spectrum of $CsCdBr_3:Yb^{3+}$, $T=4.2$ K, $c=1\%$.

$$H_{\mathrm{SO}}(nl)=\lambda_{\parallel}(nl)l_z s_z+\lambda_{\perp}(nl)(l_x s_x+l_y s_y) \tag{11}$$

(s is the electron spin moment). The CF Hamiltonian of a $4f$ electron in the symmetric dimer is determined by the six even CF parameters B_p^k:

$$H_{\mathrm{CF}}(4f)=B_2^0O_2^0+B_4^0O_4^0+B_6^0O_6^O+B_4^3O_4^3+B_6^3O_6^3+B_6^6O_6^6, \tag{12}$$

where the O_p^k are the Stevens operators corresponding to spherical polynomials formed from the directional cosines of the electron radius vector. (The reduced matrix elements are incorporated in the O_p^k). As a starting point of our analysis, we take the observed CF splitting of the states $^2F_{7/2}$ and $^2F_{5/2}$ of the $4f^{13}=4f^{14-1}$ electron configuration, which is equivalent to the eigenstates of the one-hole Hamiltonian $H(4f^{-1})$. We can expect that the CF parameters for Yb^{3+} do not differ substantially from those determined earlier for Ho^{3+}, Er^{3+}, and Tm^{3+} in the same crystal host (Table II). It has been proved that the octahedral component of the CF in the symmetric pair center dominates over the trigonal component.[1,14,23] So, we can compare the CF energies of the Yb^{3+} ions inside the deformed Br^- octahedra in the dimer centers (columns 5, 7, and 8, Table I) with those in the perfect octahedra in the elpasolites[4,24] (column 2, Table I). This comparison shows that the total CF splittings of the ^2F_J states ($J=7/2$ and 5/2) have comparable values. There is a direct correspondence between the $^2F_{7/2}1$, $^2F_{7/2}4$, and $^2F_{5/2}3$ levels of Γ_4 symmetry in the trigonal and the Γ_6 and Γ_7 doublets in the cubic field (Table I). The cubic Γ_8 quadruplets are split by the trigonal field into doublets of Γ_4 and Γ_{56} symmetry. The most remarkable difference between the energy levels in the trigonal dimer centers[2,3,17] and in the cubic centers is the pronounced downshift of the $^2F_{7/2}(\Gamma_8)$ levels in the dimers.

We found that there is no chance to achieve an agreement between the calculated and measured CF energies and g factors of the Yb^{3+} ion in the bromine coordination using the Hamiltonian (10) with reasonable values of the CF parameters. Particularly, the calculated total splitting of the excited $^2F_{5/2}$ state becomes less than the measured one by at least 150 cm^{-1}. Examples of energy-level structures calculated in the framework of the conventional CF theory are given in columns 3, 6, and 9 in Table I. For these calculations the spin-orbit coupling constants $\lambda(4f)=2911\,cm^{-1}$ for the cubic and $\lambda_{\parallel}(4f)=2913.5$, $\lambda_{\perp}(4f)=2911\,cm^{-1}$ for the trigonal centers (which are close to the free-ion value of 2918 cm^{-1})[25] and the CF parameters as given in Table II have been used. The disagreement between the calculated and measured CF energies of Yb^{3+} in the bromo elpasolites has already been noted before[4] (columns 2 and 3, Table I). A similar disagreement arose calculating the CF splittings of Er^{3+} in the iodide compound $Cs_3Y_2I_9$,[27] even going beyond the framework of the one-electron CF approximation taking into account electron correlations: The observed total splittings of the excited CF multiplets above 18 000 cm^{-1} could not be described. The reason was attributed to the configuration mixing ($4f^n$-$4f^{n-1}5d^1$) due to the decreasing energy of the $5d$ electron states in the Cl–Br–I sequence of ligands. In the cubic bromo-elpasolites, configurations of different parity cannot mix. But in the dimer centers the odd component of the CF responsible for the radiative electric dipole transitions can contribute to the CF splitting. To elucidate the role of this mechanism, we considered explicitly the effect of mixing of the ground ($4f^{13}$) and the first excited ($4f^{12}5d^1$) configurations on the CF splitting of Yb^{3+} in $CsCdBr_3$. In the free ion, the excitation energies of the 910 states belonging to the $4f^{12}5d^1$ configuration are in the range from 78 500 to 129 000 cm^{-1}.[25] Due to this large energy gap, we can neglect the inner structure of the $4f^{12}$ configuration as well as the spin-orbit and CF splittings of the $5d$ states and can calculate the energy levels of the $4f^{13}$ ground configuration considering the $4f-5d$ interaction only up to the second order. In this case the calculations can be simplified by introducing an effective one-hole Hamiltonian

$$H=H(4f^{-1})+H(5d^{-1})+H_{\mathrm{CF}}(fd), \tag{13}$$

which operates within the manifold of the twenty-four $4f$ and $5d$ states. Here

$$H_{\mathrm{CF}}(fd)=B_1^0O_1^0+B_3^0O_3^0+B_3^3O_3^3+B_5^0O_5^0+B_5^3O_5^3 \tag{14}$$

is the odd CF Hamiltonian. The parameters $B_1^0=-1232$, $B_3^0=153$, $B_3^3=-750$, $B_5^0=-82$, and $B_5^3=45\,cm^{-1}$ have been calculated in the framework of the exchange charge model[28] using the local lattice structure obtained in Ref. 1. The matrix elements $\langle 4f,l_z=m|H_{\mathrm{CF}}(fd)|5d,l_z=m\rangle$, which substitute for the matrix elements of $H_{\mathrm{CF}}(fd)$ in the space of Slater determinants, include the additional phase factor $(-1)^{m+1}$. The Hamiltonian $H(5d^{-1})$ in Eq. (13) is presented by a diagonal matrix with 10 nonzero elements equal to the parameter of the excitation energy $E(5d)=70\,000\,cm^{-1}$ of the $5d$ state relative to the reference energy $E(4f)=0$. The energies calculated from the Hamiltonian (13) are given in column 10, Table I. Comparing them with the data in column 9, Table I, obtained with the same CF parameters but without configuration mixing, shows only slight shifts of the CF levels (less than 5 cm^{-1}). The disagreement between the calculated and measured energies of the CF states, originating basically from the anomalous large splitting of the excited CF multiplet in the octahedral field, is not removed. It seems likely that this problem is related to a specific property of the ($RE^{3+}Br_6^-$) complex and that it is common to RE ions (Er^{3+}, Tm^{3+}, Yb^{3+}) having low-excitation energies of the Br–RE charge-transfer states.[19] Hence, we come to the conclusion that there have to be appreciable contributions from other interactions, especially from interactions between the Yb^{3+} ground configuration $4f^{13}$ and the charge-transfer configuration $Yb^{2+}(4f^{14})Br(4p^5)[Br^-(4p^6)]_5$ of the $(YbBr_6)^{3-}$ complex.

The Hamiltonian of this complex, operating within the manifolds of the $4f^{13}$ and $4f^{12}5d^1$ configurations of the Yb^{3+} ion and the charge-transfer states of the 36 spin orbitals of a hole in the $4p$ shells of the $6Br^-$ ions, can be written as follows (it is implicitly supposed that the one-electron wave functions are initially orthonormalized):

$$H=H(4f^{-1})+H(5d^{-1})+H_{\mathrm{CF}}(fd)+H(ch-t)+H(4f,ch-t). \tag{15}$$

The position and structure of the charge-transfer band is determined by the Hamiltonian $H(ch-t)$ represented by a matrix of dimension 36×36, which contains the gap Δ between the energy of a $4p$ hole at the ligand site and a hole in the $4f$ shell, the spin-orbit interaction in the $4p$ shell (we use the spin-orbit coupling constant of a free Br atom $\lambda(4p)=2400\,\mathrm{cm}^{-1}$),[29] the hopping integrals corresponding to the movement of a hole over the ligands, and the CF interaction at the Br sites. The Hamiltonian $H(4f,ch-t)$ corresponds to the off-diagonal terms connecting the charge-transfer states with the ground configuration. (We neglect terms that mix charge-transfer states with the excited $4f^{12}5d^1$ configuration.)

For simplicity we start with the charge-transfer states in the octahedral complex containing the RE ion in the center. The matrix of $H(ch-t)$ is constructed on the basis of the real bromine $4p$ orbitals oriented along the local coordinate axes (x_i,y_i,z_i) parallel to the tetragonal axes of the octahedron, the z_i axes directed to the center. For the ligand sites with the coordinates $(\pm R00)$ $(i=1,1')$, $(0\pm R0)$ $(i=2,2')$, $(00\pm R)$ $(i=3,3')$, we have 18 orbitals $|4px_i\rangle,|4py_i\rangle,|4pz_i\rangle$, where

$$-z_1\|z_{1'}\|-y_2\|y_{2'}\|x_3\|x_{3'}\|x;$$

$$y_1\|-y_{1'}\|-z_2\|z_{2'}\|-y_3\|y_{3'}\|y;\quad x_1\|x_{1'}\|x_2\|x_{2'}\|-z_3\|z_{3'}\|z.$$

The intersite hopping integrals are assumed to be proportional to the overlap integrals. So, for the nearest sites we have

$$\langle 4pz_1|H(ch-t)|4pz_2\rangle=-\langle 4py_1|H(ch-t)|4py_2\rangle=(J_\sigma+J_\pi)/2;$$

$$\langle 4px_1|H(ch-t)|4px_2\rangle=J_\pi; \tag{16}$$

$$-\langle 4pz_1|H(ch-t)|4py_2\rangle=\langle 4py_1|H(ch-t)|4pz_2\rangle=(J_\sigma-J_\pi)/2, \tag{17}$$

and along the octahedral body diagonals

$$\langle 4pz_1|H(ch-t)|4pz_{1'}\rangle=J'_\sigma;$$

$$\langle 4px_1|H(ch-t)|4px_{1'}\rangle=J'_\pi. \tag{18}$$

The CF terms of the $4p$ hole can be introduced using only one model parameter given by the quadrupole field component along the RE ion-ligand bond direction; particularly,

$$\langle 4px_iH|(ch-t)|4px_i\rangle=\langle 4py_i|H(ch-t)|4pzy_i\rangle=-0.5\langle 4pz_i|H(ch-t)|4pz_i\rangle=0.4B_2^0(4p). \tag{19}$$

In the point-charge approximation, taking into account the excess electron transfered onto the RE ion, we can estimate the value of the CF parameter $B_2^0(4p)=e^2\langle r^2\rangle/2R_l^3$ to be 4550 and 5650 cm^{-1} for the terminal and bridging bromine ions, respectively ($\langle r^2\rangle=0.0179\,\mathrm{nm}^2$ is the second moment of the $4p$ radial wave function presented for the bromine ion in Ref. 30, and R_l is the distance between the ligand and the RE ion). The results of the calculations presented below were obtained with the parameter $B_2^0(4p)=4125\,\mathrm{cm}^{-1}$.

The wave functions of the $4f$ and $5d$ states were used in the Yb^{3+} system of coordinates with the z axis along the trigonal axis [111] of the octahedron. The same axis was taken as quantization axis for the spin moments. To obtain the matrix elements of the spin-orbit interaction of the $4p$ holes at the bromine sites, we performed transformations of the local Br coordinates to the coordinates of the central ion. The matrix elements of the Hamiltonian $H(4f,ch-t)$ were assumed to be proportional to the overlap integrals between the $|4fm\rangle(Yb^{3+})$ and the $|4p\alpha_i\rangle$(Br) orbitals, where m corresponds to the projection of the orbital momentum on the z axis of the central ion. In particular,

$$\langle 4f3|H(4f,ch-t)|4px_1\rangle=\langle 4f3|H(4f,ch-t)|4py_1\rangle^*=T_\pi t_3;$$

$$\langle 4f3|H(4f,ch-t)|4pz_1\rangle=T_\sigma q_3, \tag{20}$$

where $t_3=\sqrt{10}(1+i\sqrt{3})/12$ and $q_3=\sqrt{30}/18$ are linear combinations of the elements of the Wigner rotation matrices $D^{(3)}_{3,\pm1}$ and $D^{(3)}_{3,0}$. Similar expressions for all other matrix elements of the Hamiltonian $H(4f,ch-t)$ were obtained by transforming the spherical harmonics $Y_{3,m}$ from the coordinates of the central ion to the local coordinates of the ligands.

The hopping integrals $T_\sigma=(536\pm14)\,\mathrm{cm}^{-1}$, $T_\pi=-(287\pm7)\,\mathrm{cm}^{-1}$ in $CsCdBr_3$:Yb^{3+} (plus and minus signs correspond to bonds with the bridging and terminal bromine ions in the pair center, respectively) and $T_\sigma=590\,\mathrm{cm}^{-1}$, $T_\pi=-205\,\mathrm{cm}^{-1}$ in $Cs_2NaHoBr_6$:Yb^{3+}, the energy gap $\Delta=12\,000\,\mathrm{cm}^{-1}$, as well as the final values of the CF parameters presented in the columns 7 and 8 of Table II, were found from fits to the experimental CF levels. The values of the parameters (cm^{-1}) $J_\sigma=200$, $J'_\sigma=20$, $J_\pi=100$, and $J'_\pi=10$ were kept fixed and used only to check the symmetry properties of the electronic wave functions. They cause only a negligible effect on the energy levels of the ground configuration. The calculated energy levels (columns 4 and 11, Table 1) obtained from our model Hamiltonian (15) agree very well with the experimental data (columns 2 and 8, Table 1). A further confirmation of the model might be obtained from optical-absorption experiments on the charge-transfer states. In the octahedral field, the charge-transfer states have the following energies (cm^{-1}) and symmetries: 12 631(nb,Γ_8), 12 987(Γ_6), 13 045(Γ_8), 13 441(nb,Γ_6), 16 895(nb,Γ_8), 16 909(Γ_7), 17 181(Γ_8), 17 365(nb,Γ_7), 19 668(nb,Γ_6), 19 885(Γ_8), 20 047(nb,Γ_8), and 20 058(Γ_6). The energy levels marked by nb correspond to spin orbitals of nonbonding type formed from $4p$ hole molecular orbitals of $a_{1g}(\sigma)$, $e_g(\sigma)$, $t_{1g}(\pi)$, and $t_{2g}(\pi)$ symmetry. Of course, the predicted positions of the charge-transfer levels are obtained using crude approximations and might not be very accurate. Corresponding absorptions may be superimposed on the broad absorption spectra of pure $CsCdBr_3$ at wave numbers higher than 20 000 cm^{-1} [1].

The CF calculations must account for the measured g factors, which are close to the isotropic g factor of the Yb^{3+} ground doublet Γ_6 in the octahedral field (column 3, Table

I). The g factors were calculated within the framework of the models introduced above taking only into account the magnetic moment of the $4f$ hole (columns 9–11, Table I). The results agree satisfactorily with the experimental data. Comparing the theoretical and experimental g factors one has to keep in mind the covalent reduction of the orbital angular momentum of the $4f$ hole. A corresponding study of covalence effects for Yb^{3+} ions in a perfect octahedral environment was presented in Ref. 31. The ground state g factor was given in the form $g(\Gamma_6)=2k_{t_1t_1}+2/3$, where $k_{t_1t_1}<1$ is the reduction for orbitals of t_{1u} symmetry. The differences of about 1.2%–3.4% between the measured and calculated g factors are in qualitative agreement with the structure of the ground-state wave function containing an admixture of 0.39% from the charge-transfer states.

IV. CONCLUSIONS

The EPR spectra in $CsCdBr_3$:Yb^{3+} crystals have shown unambiguously that most of the Yb^{3+} ions form symmetric dimer centers of the type RE^{3+}-Cd^{2+} vacancy-RE^{3+} in the octahedral $[CdBr_6]^{4-}$ chains. Contrary to the case of the Tm^{3+} and Ho^{3+} centers, where the energy of at least one of the excited CF states, determined from the optical spectra, could be found once more in the submillimeter EPR experiments, thus allowing us to identify the corresponding center by EPR techniques,[8] we have no direct arguments for the identification of the optical lines with a specific center in this paper. We assign the most intensive optical transitions to the symmetric dimers because no other impurity centers of comparable concentration could be found.

We have shown that taking into account the charge-transfer states of the quasioctahedral $(YbBr_6)^{3-}$ coordination units, it is possible to achieve a satisfactory description of the optical spectra. The data compiled in Table I demonstrate clearly the pronounced effects due to the charge-transfer states. In addition to its influence on the energy levels, the strong interaction between the $4f^{13}$ configuration and the charge-transfer states can be considered as an important mechanism for an effective interaction between the Yb^{3+} ions and the host lattice. Furthermore, this mechanism can be the reason for unusually fast and efficient nonradiative relaxation and upconversion processes in RE activated bromides. But these items are beyond the scope of the present paper.

ACKNOWLEDGMENTS

This work was supported by INTAS Grant No. N96-0232, by RFBR Grant No. N99-02-16881, and by the Academy of Sciences of Tatarstan. B.Z.M. acknowledges the support by the DFG in the framework of the Mercator Program.

[1] J. Heber, M. Lange, M. Altwein, B. Z. Malkin, and M. P. Rodionova, J. Alloys Compd. **275–277**, 181 (1998).
[2] Ph. Goldner, F. Pelle, D. Meichenin, and F. Auzel, J. Lumin. **71**, 137 (1997).
[3] M. P. Hehlen and H. U. Gudel, J. Chem. Phys. **98**, 1768 (1993).
[4] P. A. Tanner, V. V. R. K. Kumar, C. K. Jayasankar, and M. F. Reid, J. Alloys Compd. **215**, 349 (1994).
[5] N. Bodenschatz, J. Neukum, and J. Heber, J. Lumin. **66/67**, 213 (1996).
[6] J. Neukum, N. Bodenschatz, and J. Heber, Phys. Rev. B **50**, 3536 (1994).
[7] L. M. Henling and G. L. McPherson, Phys. Rev. B **16**, 4756 (1977).
[8] V. F. Tarasov, G. S. Shakurov, B. Z. Malkin, A. I. Iskhakova, J. Heber, and M. Altwein, Pis'ma Zh. Eksp. Teor. Fiz. **65**, 535 (1997) [JETP Lett. **65**, 559 (1997)].
[9] N. J. Cockroft, G. D. Jones, and R. W. G. Syme, J. Lumin. **43**, 275 (1989).
[10] C. Bartout and R. B. Barthem, J. Lumin. **46**, 9 (1990).
[11] M. Mujaji, G. D. Jones, and R. W. G. Syme, Phys. Rev. B **48**, 710 (1993).
[12] Ph. Goldner and F. Pelle, J. Lumin. **55**, 197 (1993).
[13] F. Pelle, N. Gardant, M. Genotelle, Ph. Goldner, and P. Porcher, J. Phys. Chem. Solids **56**, 1003 (1995).
[14] B. Z. Malkin, A. I. Ishakova, V. F. Tarasov, G. S. Shakurov, J. Heber, and M. Altwein, J. Alloys Compd. **275–277**, 209 (1998).
[15] E. Antic-Fidancev, M. Lemaitre-Blaise, J-P. Chaminade, and P. Porcher, J. Alloys Compd. **225**, 95 (1995).
[16] J. R. Quagliano, N. J. Cockroft, K. E. Gunde, and F. S. Richardson, J. Chem. Phys. **105**, 9812 (1996).
[17] M. P. Hehlen, A. Kuditcher, S. C. Rand, and M. A. Tischler, J. Chem. Phys. **107**, 4886 (1997).
[18] B. Judd, J. Phys. C **13**, 2695 (1980).
[19] G. Ionova, J. C. Krupa, I. Gerard, and R. Guillaumont, New J. Chem. **19**, 677 (1995).
[20] J. M. Baker, W. B. Blake, and G. M. Copland, Proc. R. Soc. London, Ser. A **309**, 119 (1969).
[21] M. A. H. McCausland and I. S. Mackenzie, Adv. Phys. **28**, 305 (1979).
[22] A. Donni, A. Furrer, and H. U. Gudel, J. Solid State Chem. **81**, 278 (1989).
[23] F. Ramaz, R. M. Macfarlane, J. C. Vial, J. P. Chaminade, and F. Madeore, J. Lumin. **55**, 173 (1993).
[24] A. Furrer and H. U. Gudel, Phys. Rev. B **56**, 15 062 (1997).
[25] W. C. Martin, R. Zalubas, and L. Hagan, *Atomic Energy Levels—The Rare-Earth Elements* (National Bureau of Standards, Washington, 1978).
[26] M. P. Hehlen, H. U. Gudel, and J. R. Quagliano, J. Chem. Phys. **101**, 10 303 (1994).
[27] S. R. Luthi, H. U. Gudel, and M. P. Hehlen, J. Chem. Phys. **110**, 12 033 (1999).
[28] B. Z. Malkin, in *Spectroscopy of Solids Containing Rare-Earth Ions*, edited by A. A. Kaplyanskii and R. M. Macfarlane (North-Holland, Amsterdam, 1987), p. 13.
[29] C. E. Moore, *Atomic Energy Levels*, Nat. Stand. Ref. Data Ser. 35 (National Bureau of Standards, Washington, DC, 1971), Vols. 1, 2, and 3.
[30] E. Clementi and C. R. Roetti, At. Data Nucl. Data Tables **14**, N3–4 (1974).
[31] J. H. M. Thornley, Proc. Phys. Soc. London **88**, 325 (1966).